

# Detection of Generalized Media-based Modulation Signals using Multi-layered Message Passing

Manu Krishnan K., Swaroop Jacob<sup>†</sup>, and A. Chockalingam  
Department of ECE, Indian Institute of Science, Bangalore-560012  
<sup>†</sup> Presently with Cisco Systems India Pvt. Ltd., Bangalore-560087

**Abstract**—In this paper, we consider generalized media-based modulation (GMBM) where transmit antennas and RF mirrors (which are parasitic elements placed near the transmit antennas as digitally controlled scatterers) are indexed simultaneously to convey information bits. GMBM systems offer the advantages of high rates, reduced transmit RF hardware complexity, and improved performance compared to conventional multi-antenna systems. This paper focuses on the detection of large-scale GMBM signals, where maximum-likelihood detection is not feasible due to its exponential complexity in the transmit rate. Message passing based detection is a promising low-complexity approach. However, message passing over a bipartite graph is not possible in GMBM signal detection because the elements of the GMBM transmit vector are interdependent. Our new contribution in this paper is that we propose a *multi-layered message passing (MLMP) algorithm* that decouples the dependencies through the addition of new layers and constraints that account for the antenna activation and RF mirror activation patterns. The proposed MLMP algorithm is shown to scale well in complexity and also to achieve good bit error performance in high-rate large-dimension systems.

**Keywords** – Media-based modulation (MBM), RF mirrors, generalized MBM, multi-layered message passing.

## I. INTRODUCTION

Media-based modulation (MBM) has recently started drawing research attention as a promising modulation scheme for high data rate wireless communication in rich scattering environments. In MBM, digitally controlled parasitic elements are employed as radio frequency (RF) mirrors to influence the local scattering environment near the transmit antennas [1]-[7]. An incoming stream of information bits decides the ON/OFF configuration of the RF mirrors, which, in turn, creates different channel fade realizations. Mirrors in the ON status reflect the RF signal, and those in the OFF status allow the signal to pass through. The basic idea behind the MBM scheme is explained as follows. RF mirrors are placed near a transmit antenna to alter the propagation media surrounding the antenna based on the ON/OFF status of the mirrors. In rich scattering environments, small perturbations in the near field at the transmitter lead to independent channel fade realizations in the far field at the receiver. Each permutation of the ON/OFF status of the mirrors is called a mirror activation pattern (MAP). If there are  $m_{\text{rf}}$  mirrors,  $2^{m_{\text{rf}}}$  different MAPs are possible. One of the  $2^{m_{\text{rf}}}$  MAPs is selected by the transmitter based on  $m_{\text{rf}}$  information bits. The channel fade realization corresponding to the selected MAP conveys the  $m_{\text{rf}}$  information bits. In addition, a symbol chosen from a conventional modulation alphabet (e.g., QAM/PSK) transmitted by the antenna also

conveys information bits. A key attraction in MBM is its high achievable rate that increases linearly in the number of RF mirrors.

A comprehensive description of MBM in comparison with other index modulation schemes such as space shift keying (SSK) and spatial modulation (SM) is presented in [4]. The thrust for research in MBM comes from the results in [2], which show that MBM with  $n_r$  receive antennas is capable of asymptotically (for large  $m_{\text{rf}}$ ) achieving the capacity of  $n_r$  parallel AWGN channels. This is particularly interesting because the RF hardware complexity of the MBM transmitter is small as RF mirrors do not need transmit RF chains to activate them. Developing practical receiver techniques/algorithms for detection of MBM signals at the receiver, however, is crucial to reap the high-rate and low-RF hardware complexity advantages of MBM. This forms the main focus in this paper.

In this paper, we focus on generalized MBM (GMBM) scheme which has the potential to achieve very high rates through indexing of both transmit antennas as well as RF mirrors. Generalized spatial modulation (GSM) [8]-[10] is a multi-antenna modulation scheme, where a subset of the available transmit antennas are made active at a time and symbols from a QAM/PSK alphabet are transmitted on the active antennas. The combination of antennas in the active subset also conveys information bits. In GMBM, multiple antennas and RF mirrors near each antenna are used, and information bits are conveyed through indexing of antennas, indexing of RF mirrors in each active antenna, and QAM/PSK symbols. Since maximum-likelihood (ML) detection becomes impractical for large-scale GMBM signals, we consider a message passing approach for GMBM signal detection. Specifically, we propose a *multi-layered message passing (MLMP) algorithm* for the detection of point-to-point GMBM signals. The elements in a GMBM signal vector are interdependent because of which message passing over a bipartite graph is not possible. To address this, a multi-layering component and additional constraints are proposed in the message passing approach to decouple the dependencies. Messages are iteratively passed over the multiple layers. The proposed algorithm is shown to scale well in complexity and also to achieve good bit error performance in high-rate large-dimension GMBM systems.

## II. GMBM SYSTEM MODEL

The GMBM transmitter is shown in Fig. 1. An MBM transmit unit (MBM-TU) consists of a transmit antenna and  $m_{\text{rf}}$  RF mirrors surrounding it. Consider a system having  $n_{\text{tu}}$  MBM-TUs at the transmit side and  $n_r$  antennas at the receive side. The  $n_{\text{tu}}$  MBM-TUs are fed by  $n_{\text{rf}}$  RF chains

This work was supported in part by the J. C. Bose National Fellowship, Department of Science and Technology, Government of India.

( $1 \leq n_{\text{rf}} \leq n_{\text{tu}}$ ) through an  $n_{\text{rf}} \times n_{\text{tu}}$  RF switch. Out of the  $n_{\text{tu}}$  MBM-TUs,  $n_{\text{rf}}$  MBM-TUs are activated at a time. So there are  $\binom{n_{\text{tu}}}{n_{\text{rf}}}$  possible combinations of active MBM-TUs. Each combination is called a MBM-TU activation pattern (MTAP). Out of the  $\binom{n_{\text{tu}}}{n_{\text{rf}}}$  MTAPs,  $2^{\lfloor \log_2 \binom{n_{\text{tu}}}{n_{\text{rf}}} \rfloor}$  MTAPs are used for signaling which conveys  $\lfloor \log_2 \binom{n_{\text{tu}}}{n_{\text{rf}}} \rfloor$  bits through indexing of MBM-TUs. There are  $m_{\text{rf}}$  RF mirrors that can be controlled in each of the active MBM-TU. The ON/OFF status of each mirror is controlled by one information bit. Each permutation of the ON/OFF status of the  $m_{\text{rf}}$  mirrors in an active MBM-TU is called a mirror activation pattern (MAP); note that  $N_{\text{m}} = 2^{m_{\text{rf}}}$  MAPs are possible in an active MBM-TU. Thus,  $n_{\text{rf}}m_{\text{rf}}$  bits are conveyed through indexing of mirrors. Also, each active MBM-TU transmits an  $M$ -ary QAM/PSK symbol conveying  $\log_2 M$  bits. Thus, the transmission rate is

$$\eta = \lfloor \log_2 \binom{n_{\text{tu}}}{n_{\text{rf}}} \rfloor + n_{\text{rf}}m_{\text{rf}} + n_{\text{rf}} \log_2 |\mathbb{A}| \text{ bpcu}. \quad (1)$$

### A. MBM channel alphabet

Let  $\mathbf{h}_l^k$  denote the  $n_r \times 1$  channel vector at the receiver corresponding to the  $k$ th MAP of the  $l$ th MBM-TU, where  $\mathbf{h}_l^k = [h_{1,l}^k, h_{2,l}^k, \dots, h_{n_r,l}^k]^T$ ,  $h_{j,l}^k \sim \mathcal{CN}(0,1)$  being the channel fade seen by the  $j$ th receive antenna when the  $k$ th MAP of the  $l$ th MBM-TU is active,  $j = 1, \dots, n_r$ ,  $l = 1, \dots, n_{\text{tu}}$ ,  $k = 1, \dots, N_{\text{m}}$ , and  $N_{\text{m}} \triangleq 2^{m_{\text{rf}}}$ . The set of the vectors  $\mathbb{H}_l = \{\mathbf{h}_l^1, \mathbf{h}_l^2, \dots, \mathbf{h}_l^{N_{\text{m}}}\}$  is the channel alphabet corresponding to the  $l$ th MBM-TU at the receiver. Thus,  $\mathbb{H} = [\mathbb{H}_1, \mathbb{H}_2, \dots, \mathbb{H}_{n_{\text{tu}}}]$  is the channel alphabet of the system.

### B. GMBM signal set

Let the set of MTAPs used be for signalling be denoted by  $\mathbb{S}_a$ . Different combinations of  $\lfloor \log_2 \binom{n_{\text{tu}}}{n_{\text{rf}}} \rfloor$  bits are mapped to unique patterns in  $\mathbb{S}_a$ . Let  $\mathbb{S}_{\text{gsm}}$  denote the GSM signal set consisting of  $n_{\text{tu}} \times 1$  GSM signal vectors [9]:

$$\mathbb{S}_{\text{gsm}} = \{\mathbf{s} : s_i \in \mathbb{A} \cup \{0\}, \|\mathbf{s}\|_0 = n_{\text{rf}}, \mathcal{I}(\mathbf{s}) \in \mathbb{S}_a\}, \quad (2)$$

where  $\mathbb{A}$  is the  $M$ -ary QAM/PSK alphabet,  $s_i$  is the  $i$ th element of  $\mathbf{s}$ ,  $i = 1, 2, \dots, n_{\text{tu}}$ ,  $\|\mathbf{s}\|_0$  is the  $l_0$ -norm of the GSM signal vector  $\mathbf{s}$ , and  $\mathcal{I}(\mathbf{s})$  gives the MTAP corresponding to  $\mathbf{s}$ . Now, the GMBM signal set is defined as

$$\mathbb{S}_{\text{gmbm}} = \{\mathbf{x} = [\mathbf{x}_1^T \mathbf{x}_2^T \dots \mathbf{x}_{n_{\text{tu}}}^T]^T : \mathbf{x}_i = s_i \mathbf{e}_{l_i}, l_i \in \{1, \dots, N_{\text{m}}\}; \mathbf{s} = [s_1 s_2 \dots s_{n_{\text{tu}}}]^T \in \mathbb{S}_{\text{gsm}}\}, \quad (3)$$

where  $\mathbf{e}_{l_i}$  is an  $N_{\text{m}} \times 1$  vector whose  $l_i$ th coordinate is 1 and all other coordinates are zeros.

### C. Received GMBM signal

Let  $\mathbf{H}_i = \{\mathbf{h}_i^1, \mathbf{h}_i^2, \dots, \mathbf{h}_i^{N_{\text{m}}}\}$  denote the channel matrix corresponding to the  $i$ th MBM-TU. The received vector  $\mathbf{y}$  is given by

$$\mathbf{y} = \sum_{i=1}^{n_{\text{tu}}} s_i \mathbf{H}_i \mathbf{e}_{l_i} + \mathbf{n}, \quad (4)$$

where  $\mathbf{n} \sim \mathcal{CN}(0, \sigma^2 \mathbf{I}_{n_r})$  is the AWGN noise vector. Defining  $\mathbf{H} = [\mathbf{H}_1 \mathbf{H}_2 \dots \mathbf{H}_{n_{\text{tu}}}]$ , we can write (4) as

$$\mathbf{y} = \mathbf{H}\mathbf{x} + \mathbf{n}. \quad (5)$$

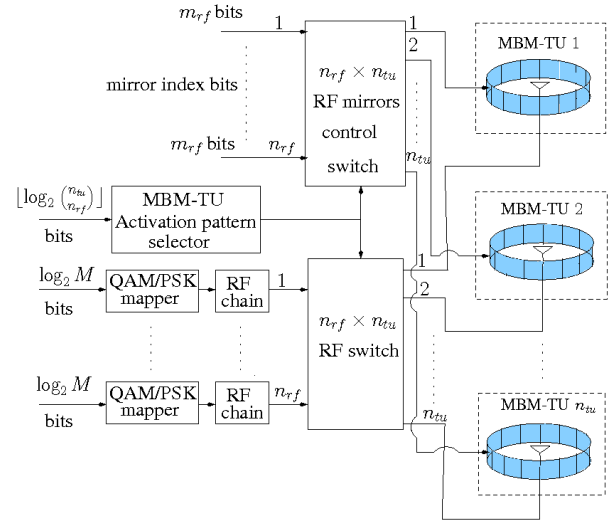


Fig. 1. GMBM transmitter model.

Now, the ML detection rule is given by

$$\hat{\mathbf{x}} = \underset{\mathbf{x} \in \mathbb{S}_{\text{gmbm}}}{\operatorname{argmin}} \|\mathbf{y} - \mathbf{H}\mathbf{x}\|^2, \quad (6)$$

which has exponential complexity. We propose a message passing based low-complexity detection algorithm in the next section.

## III. DETECTION USING MULTI-LAYERED MESSAGE PASSING

The elements of the GMBM transmit vector are interdependent due to indexing the MBM-TUs and the RF mirrors. We decouple the elements by introducing two new layers to account for the MAP and the MTAP. Mapping of information bits to MTAPs is done using combinadics [10]. The maximum a posteriori probability (APP) decision rule for GMBM signal detection is given by

$$\hat{\mathbf{x}} = \underset{\mathbf{x} \in \mathbb{S}_{\text{gmbm}}}{\operatorname{argmax}} p(\mathbf{x}|\mathbf{y}), \quad (7)$$

where  $p(\mathbf{x}|\mathbf{y})$  can be written as

$$\begin{aligned} p(\mathbf{x}, \mathbf{m}, \mathbf{a}|\mathbf{y}) &\propto p(\mathbf{y}|\mathbf{x}, \mathbf{m}, \mathbf{a})p(\mathbf{x}, \mathbf{m}, \mathbf{a}) \\ &= p(\mathbf{y}|\mathbf{x})p(\mathbf{x}|\mathbf{m})p(\mathbf{m}|\mathbf{a})p(\mathbf{a}) \\ &= \left\{ \prod_{j=1}^{n_r} p(y_j|\mathbf{x}) \prod_{k=1}^{n_{\text{tu}}N_{\text{m}}} p(x_k|m_k) \prod_{i=1}^{n_{\text{tu}}} \prod_{l=(i-1)N_{\text{m}}+1}^{iN_{\text{m}}} p(m_l|a_i) \right\} p(\mathbf{a}). \end{aligned} \quad (8)$$

In (8),  $\mathbf{m} = [m_1, m_2, \dots, m_{n_{\text{tu}}N_{\text{m}}}]$  and  $\mathbf{a} = [a_1, a_2, \dots, a_{n_{\text{tu}}}]$  account for the MAPs and the MTAP, respectively. Thus, by introducing the  $\mathbf{m}$  and  $\mathbf{a}$  layers, we have decoupled the elements of the transmit vector  $\mathbf{x}$ . In view of (8), we model the GMBM system as a graph illustrated in Fig. 2, with the following six types of nodes:

- $n_r$  observation nodes corresponding to elements of  $\mathbf{y}$ .
- $n_{\text{tu}}N_{\text{m}}$  variable nodes corresponding to elements of  $\mathbf{x}$ .
- $n_{\text{tu}}N_{\text{m}}$  MAP indicator nodes  $m_i$ ,  $1 \leq i \leq n_{\text{tu}}N_{\text{m}}$ .
- $n_{\text{tu}}$  MAP constraint nodes  $M_i$ ,  $1 \leq i \leq n_{\text{tu}}$ .

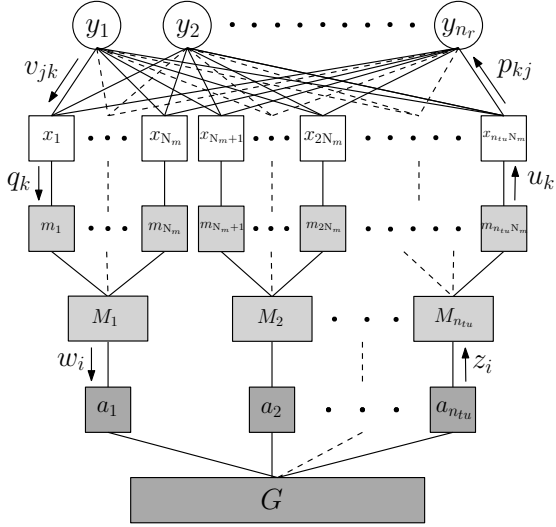


Fig. 2. Graphical model and the messages passed in the proposed MLMP detector.

- $n_{tu}$  MTAP indicator nodes  $a_i$ ,  $1 \leq i \leq n_{tu}$ .
- a MTAP constraint node  $G$ .

Note that the MAP indicator  $m_k = 1$  when  $x_k = x \in \mathbb{A}$  and 0 otherwise. The MTAP indicator  $a_i = 1$  when the MAP constraint  $M_i$  is active, i.e.,  $\sum_{l=(i-1)N_m}^{iN_m} m_l = 1$ . The MTAP constraint  $G$  is  $\sum_{i=1}^{n_{tu}} a_i = n_{rf}$ .

We use a Gaussian approximation of the interference terms to construct the messages, and iteratively pass these messages on the graph to obtain approximate marginal probabilities of the transmitted symbols. As seen in Fig. 2, three layers of message passing are involved as explained below.

From (5), we have

$$y_j = h_{jk}x_k + \underbrace{\sum_{\substack{l=1 \\ l \neq k}}^{n_{tu}N_m} h_{jl}x_l}_{\triangleq g_{jk}} + n_j, \quad (9)$$

where  $j = 1, \dots, n_r$  and  $k = 1, \dots, n_{tu}N_m$ . We approximate  $g_{jk}$  in (9) as Gaussian with mean  $\mu_{jk}$  and variance  $\sigma_{jk}^2$ , given by

$$\mu_{jk} = \sum_{\substack{l=1 \\ l \neq k}}^{n_{tu}N_m} h_{jl} \sum_{x \in \mathbb{A} \cup \mathbb{O}} x p_{lj}(x), \quad (10)$$

$$\sigma_{jk}^2 = \sum_{\substack{l=1 \\ l \neq k}}^{n_{tu}N_m} |h_{jl}|^2 \left( \sum_{x \in \mathbb{A} \cup \mathbb{O}} |x|^2 p_{lj}(x) - \left( \sum_{x \in \mathbb{A} \cup \mathbb{O}} x p_{lj}(x) \right)^2 \right) + \sigma^2. \quad (11)$$

*Layer 1:* The message  $v_{jk}$  is the probability estimate of the element  $x_k$  passed from observation node  $y_j$  to variable node  $x_k$ , given by

$$v_{jk}(x) \triangleq \Pr(x_k = x | y_j) \approx \frac{1}{\pi \sigma_{jk}^2} \exp\left(-\frac{|y_j - \mu_{jk} - h_{jk}x|^2}{\sigma_{jk}^2}\right). \quad (12)$$

Likewise, the message  $p_{kj}$  is the APP estimate of the element of  $\mathbf{x}$  passed from variable node  $x_k$  to observation node  $y_j$ , given by

$$p_{kj}(x) \triangleq \Pr(x_k = x | \mathbf{y}_{\setminus j}) \approx \prod_{\substack{l=1 \\ l \neq j}}^{n_r} \Pr(x_k = x | y_l) \propto u_k(x^\odot) \prod_{\substack{l=1 \\ l \neq j}}^{n_r} v_{lk}(x), \quad (13)$$

where  $\mathbf{y}_{\setminus j}$  is the set of observation nodes excluding  $y_j$ , and

$$x^\odot = \begin{cases} 0 & x = 0 \\ 1 & x \in \mathbb{A}. \end{cases}$$

*Layer 2:* The message  $q_k$  is the APP of  $m_k$ , passed from variable node  $x_k$  to MAP indicator node  $m_k$ , given by

$$\begin{aligned} q_k(b) &\triangleq \Pr(m_k = b | \mathbf{x}) \\ &\approx \begin{cases} \sum_{x \in \mathbb{A}} \prod_{l=1}^{n_r} \Pr(x_k = x | y_l), & \text{if } b = 1 \\ \prod_{l=1}^{n_r} \Pr(x_k = 0 | y_l), & \text{if } b = 0 \end{cases} \\ &\propto \begin{cases} \sum_{x \in \mathbb{A}} \prod_{l=1}^{n_r} v_{lk}(x), & \text{if } b = 1 \\ \prod_{l=1}^{n_r} v_{lk}(0), & \text{if } b = 0. \end{cases} \end{aligned} \quad (14)$$

Similarly,  $u_k$  is the message from MAP indicator node  $m_k$  to variable node  $x_k$  after processing the MAP constraints  $M_i$ , given by

$$\begin{aligned} u_k(b) &\triangleq \Pr(m_k = b | \mathbf{x}_{\setminus k}^i) \\ &\propto \begin{cases} \Pr\left(\sum_{\substack{l=(i-1)N_m+1 \\ l \neq k}}^{iN_m} m_l = 0 | \mathbf{m}_{\setminus k}^i\right), & \text{if } b = 1 \\ \Pr\left(\sum_{\substack{l=(i-1)N_m+1 \\ l \neq k}}^{iN_m} m_l = 1 | \mathbf{m}_{\setminus k}^i\right), & \text{if } b = 0 \end{cases} \\ &\approx \begin{cases} \phi_k(0), & \text{if } b = 1 \\ \phi_k(1), & \text{if } b = 0, \end{cases} \end{aligned} \quad (15)$$

where  $\mathbf{x}^i = [x_{(i-1)N_m+1}, x_{(i-1)N_m+2}, \dots, x_{iN_m}]$ ,  $\mathbf{x}_{\setminus k}^i$  denotes  $\mathbf{x}^i$  excluding  $x_k$  for  $k \in [(i-1)N_m+1, (i-1)N_m+2, \dots, iN_m]$ ,  $i = 1, 2, \dots, n_{tu}$ , and  $\phi_k$  is the APP estimate of  $m_k$  which involves the summation of  $N_m - 1$  random variables. It is evaluated as  $\phi_k = \otimes_{\substack{l=(i-1)N_m+1 \\ l \neq k}}^{iN_m} z_i(1) \mathbf{q}_l$ , where  $\otimes$  is the convolution operator,  $\mathbf{q}_l = [q_l(0) \ q_l(1)]$ , and  $z_i(1)$  is the APP of  $i$ th MBM-TU being active after processing the MTAP constraint.

*Layer 3:* The message  $w_i$  is the APP estimate of MTAP indicator  $a_i$  from MAP constraint node  $M_i$ , given by

$$\begin{aligned} w_i(b) &= \Pr(a_i = b | \mathbf{m}^i) \\ &= \begin{cases} \sum_{l=(i-1)N_m+1}^{iN_m} q_l(1) \prod_{\substack{r=(i-1)N_m+1 \\ r \neq l}}^{iN_m} q_r(0), & \text{if } b = 1 \\ \prod_{l=(i-1)N_m+1}^{iN_m} q_l(0), & \text{if } b = 0. \end{cases} \end{aligned} \quad (16)$$

The message  $z_i$  is the probability estimate of MTAP indicator  $a_i$  passed from node  $a_i$  to the MAP constraint node  $M_i$  after processing the MTAP constraint  $G$ , given by

$$\begin{aligned} z_i(b) &= \Pr(a_i = b | \mathbf{a}_{\setminus i}) \\ &= \begin{cases} \Pr\left(\sum_{\substack{l=1 \\ l \neq i}}^{n_t} a_l = n_{rf} - 1 | \mathbf{a}_{\setminus i}\right), & \text{if } b = 1 \\ \Pr\left(\sum_{\substack{l=1 \\ l \neq i}}^{n_t} a_l = n_{rf} | \mathbf{a}_{\setminus i}\right), & \text{if } b = 0 \end{cases} \\ &\approx \begin{cases} \psi_i(n_{rf} - 1), & \text{if } b = 1 \\ \psi_i(n_{rf}), & \text{if } b = 0, \end{cases} \end{aligned} \quad (17)$$

where  $\psi_i = \bigotimes_{l=1}^{n_{tu}} \mathbf{w}_l$  and  $\mathbf{w}_l = [w_l(0) \ w_l(1)]$ .

The message passing algorithm is summarized as follows:

- 1) Initialize  $p_{k,j}(x) = \frac{1}{|\mathbb{A} \cup 0|}$ ,  $q_k(1) = \frac{1}{N_m}$ ,  $q_k(0) = 1 - \frac{1}{N_m}$   
 $z_i(1) = \frac{n_{rf}}{n_t}$ ,  $z_i(0) = 1 - \frac{n_{rf}}{n_t} \forall x, i, j, k$
- 2) Compute  $v_{j,k}(x), \forall x, j, k$ .
- 3) Compute  $u_k(b), \forall b, k$ .
- 4) Compute  $p_{k,j}(x), \forall x, j, k$ .
- 5) Compute  $q_k(b), \forall b, k$ .
- 6) Compute  $w_i(b), \forall b, i$ .
- 7) Compute  $z_i(b), \forall b, i$ .

Damping of the messages  $p_{k,j}(x)$  and  $q_k(b)$  is done with a damping factor  $\Delta \in (0, 1)$  to improve convergence [11]. After completing sufficient number of iterations for convergence of the messages, we get the APP estimate of each element of the transmit vector  $\mathbf{x}$  as

$$\Pr(x_k = x) = \frac{1}{C} u_k(x^\circ) \prod_{l=1}^{n_r} v_{lk}(x), \forall x \in \mathbb{A} \cup 0, \quad (18)$$

where  $C$  is a normalizing constant. Now, demapping is done as follows.

- 1) From  $z_1(1), z_2(1), \dots, z_{n_{tu}}(1)$ , find  $n_{rf}$  leading values. The index set of the leading values will give the index of the active MBM-TUs (i.e., the MTAP). Thus,  $\lfloor \log_2 \binom{n_{tu}}{n_{rf}} \rfloor$  bits of information are demapped.
- 2) Let  $[l_1, l_2, \dots, l_{n_{rf}}]$  be the index set of active MBM-TUs. Consider the MBM-TU  $n_{l_1}$ . Find  $(\hat{r}, \hat{x}_{l_1}) = \arg \max_{r,x} \Pr(x_r = x)$ , where  $r \in [(l_1 - 1)N_m + 1, (l_1 - 1)N_m + 2, \dots, l_1 N_m]$  and  $x \in \mathbb{A} \cup 0$ .  $\hat{r}$  gives the index of the active mirrors, giving the corresponding  $m_{rf}$  bits.  $\hat{x}_{l_1}$  is the detected symbol which gives  $\log_2 |\mathbb{A}|$  bits. This procedure is repeated for all the active MBM-TUs and the respective mirror index bits and symbols are demapped.

*Computational complexity:* The ML detection in (6) has exponential complexity. In the MLMP algorithm, equations (12), (15) and (17) have computational complexities of the order of  $O(n_r n_{tu} N_m |\mathbb{A}|)$ ,  $O(n_{tu} (N_m^2 + N_m))$  and  $O(n_{tu}^2 + n_{tu})$  respectively, per iteration. For  $n_r > n_{tu}$  and  $n_r > N_m$ ,  $O(n_r n_{tu} N_m |\mathbb{A}|)$  dominates over the other terms and is hence the order of complexity of the algorithm. This is significantly lower compared to that of ML and scales well for large-scale GMBM signal detection as illustrated in Fig. 3. Figure 3 shows the computational complexity in number of real operations as a function of (a)  $m_{rf}$  for  $n_{tu} = 4, 16$  with  $n_{rf} = 4$ , 4-QAM, and  $n_r = 64$  and (b)  $n_{tu}$  for  $m_{rf} = 2, 4$  with  $n_{rf} = 4$ , 4-QAM, and  $n_r = 64$ . The illustration strengthens the fact that MLMP detection is computationally more efficient than ML detection.

#### IV. RESULTS AND DISCUSSIONS

In this section, we present the simulated BER performance of the proposed MLMP algorithm. The number of iterations and damping factor used in the MLMP algorithm are 10 and 0.3, respectively. First, in Fig. 4, we present the BER performance of the proposed MLMP detection with that of ML detection in a GMBM system with the  $m_{rf} = 2$ ,  $n_r = 16$ ,

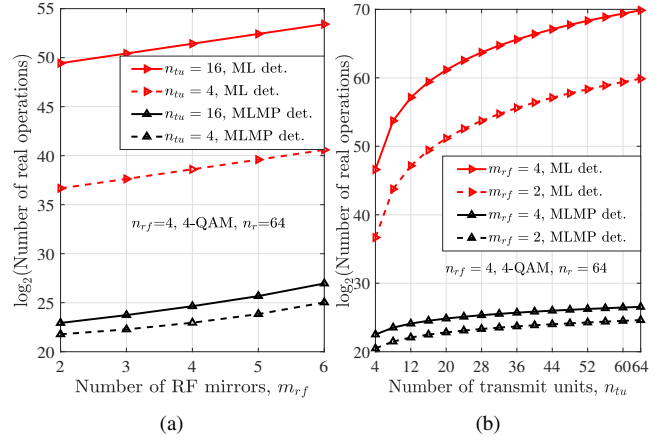


Fig. 3. Computational complexity of ML and MLMP detection algorithms in number of real operations as a function of (a)  $m_{rf}$  for  $n_{tu} = 4, 16$  with  $n_{rf} = 4$ , 4-QAM, and  $n_r = 64$  (b)  $n_{tu}$  for  $m_{rf} = 2, 4$  with  $n_{rf} = 4$ , 4-QAM, and  $n_r = 64$ .

4-QAM, and 10 bpcu. The performance achieved by MMSE detection is also shown for comparison. It can be seen that the MLMP algorithm achieves a BER of  $10^{-5}$  at an SNR which is only about 2 dB more compared to ML performance. This is indeed a very good performance for a suboptimal algorithm with polynomial complexity. Note that the performance of MMSE detection is significantly poorer compared to that of the proposed MLMP algorithm.

Having illustrated the nearness of the MLMP performance to ML performance in a moderate-dimension system in Fig. 4 (dimension of  $\mathbf{x}$  vector in this case is  $n_{tu} 2^{m_{rf}} = 4 \times 2^2 = 16$ ), we next illustrate the MLMP performance in large-dimension systems in which ML detection is complexity-wise prohibitive. Hence, only MMSE detection performance is shown for comparison. Figure 5 shows the BER performance of a GMBM system with  $n_{tu} = 8$ ,  $n_{rf} = 4$ ,  $n_r = 48$ ,  $m_{rf} = 4$ , 4-QAM, and 30 bpcu. Note that rate is high (30 bpcu) and the dimension of the  $\mathbf{x}$  vector in this case is large ( $n_{tu} 2^{m_{rf}} = 8 \times 2^4 = 128$ ). ML detection is clearly prohibitive for this system size. From Fig. 5, we can see that while the proposed MLMP and MMSE are comparable in complexity, performance-wise MLMP detection is far superior compared to MMSE detection.

Next, Fig. 6 shows the effect of increasing the rate on the performance of MLMP detection. The parameters considered in Fig. 6 are  $n_{tu} = 16$ ,  $n_{rf} = 8$ ,  $m_{rf} = 2$ , and 4-QAM, resulting in a rate of 45 bpcu. The dimension of the  $\mathbf{x}$  vector in this case is 64 ( $n_{tu} 2^{m_{rf}} = 16 \times 2^2 = 64$ ). Even in this higher rate system, MLMP performs very well and achieves a significantly better performance compared to MMSE performance.

Finally, we illustrate the effect of varying the number of receive antennas  $n_r$ . In Fig. 7, we plot the the SNR required to achieve a target BER of  $10^{-3}$  as a function  $n_r$  for the GMBM systems considered previously. The parameters of the two considered systems were: (i) system 1 with  $n_{tu} = 8$ ,  $n_{rf} = 4$ ,  $m_{rf} = 4$ , 4-QAM, 30 bpcu and (ii) system 2 with  $n_{tu} = 16$ ,  $n_{rf} = 8$ ,  $m_{rf} = 2$ , 4-QAM, 45 bpcu. As expected, in both the systems, the SNR required to achieve the target BER diminishes as  $n_r$  increases. For example, in system 2, with

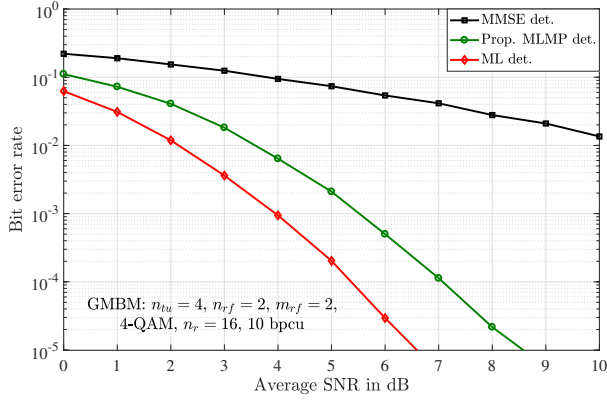


Fig. 4. BER performance comparison among the proposed MLMP detection, ML detection, and MMSE detection in a GGBM system with  $n_{tu} = 4$ ,  $n_{rf} = 2$ ,  $m_{rf} = 2$ ,  $n_r = 16$ , 4-QAM, and 10 bpcu.

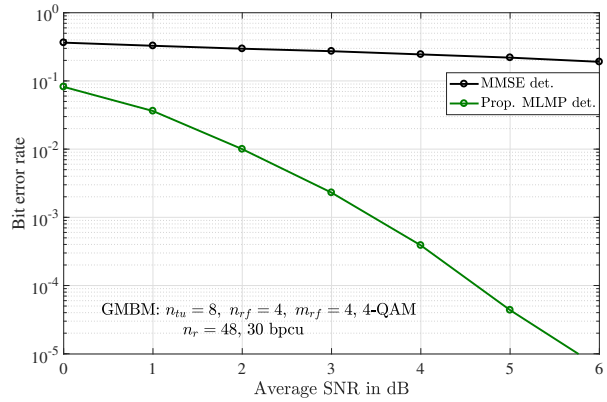


Fig. 5. BER performance of the proposed MLMP detection and MMSE detection in a system with  $n_{tu} = 8$ ,  $n_{rf} = 4$ ,  $m_{rf} = 4$ ,  $n_r = 48$ , 4-QAM, and 30 bpcu.

$n_r = 36$ ,  $10^{-3}$  BER is achieved at an SNR of about 14 dB, whereas, with  $n_r = 72$ , the SNR required drops to about 4 dB, i.e., doubling  $n_r$  has resulted in 10 dB gain in SNR. However, as can be seen from the figure, there is a diminishing returns in the SNR gain with increasing  $n_r$  because AWGN noise becomes the limiting factor.

## V. CONCLUSIONS

We proposed a low-complexity message passing based algorithm for efficient detection of high-rate large-dimension point-to-point GGBM signals. The key enablers of good performance at low complexities in the proposed algorithm are: 1) the decoupling of the dependencies in the elements of the GGBM signal vector through the addition of multiple layers and constraints to account for the antenna and mirror activation patterns in the graphical model that defines the system, and 2) the use of Gaussian approximation of the interference terms in constructing the messages to be passed across these layers. Simulation results showed that the proposed MLMP algorithm achieved good bit error performance at low complexities.

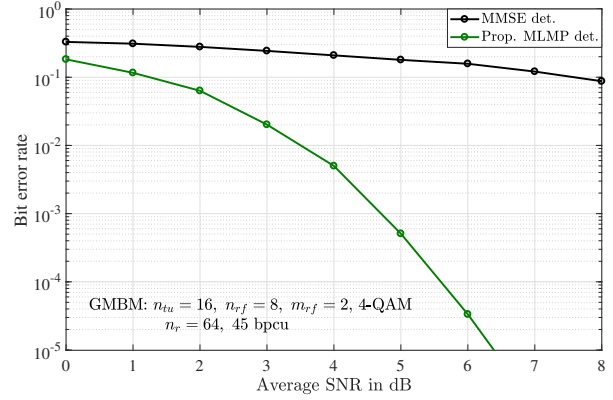


Fig. 6. BER performance of MLMP detection and MMSE detection in a GGBM system with  $n_{tu} = 16$ ,  $n_{rf} = 8$ ,  $n_r = 64$ ,  $m_{rf} = 2$ , 4-QAM, and 45 bpcu.

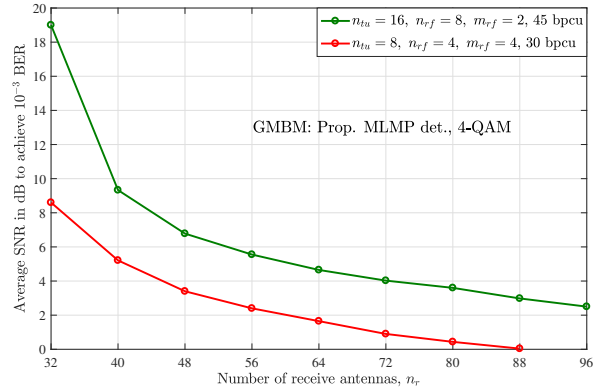


Fig. 7. Average SNR required to achieve  $10^{-3}$  BER as a function of  $n_r$  with MLMP detection and 4-QAM in two GGBM systems: (i)  $n_{tu} = 8$ ,  $n_{rf} = 4$ ,  $m_{rf} = 4$ , 30 bpcu and (ii)  $n_{tu} = 16$ ,  $n_{rf} = 8$ ,  $m_{rf} = 2$ , 45 bpcu.

## REFERENCES

- [1] A. K. Khandani, "Media-based modulation: a new approach to wireless transmission," *Proc. IEEE ISIT'2013*, pp. 3050-3054, Jul. 2013.
- [2] A. K. Khandani, "Media-based modulation: converting static Rayleigh fading to AWGN," *Proc. IEEE ISIT'2014*, pp. 1549-1553, Jun./Jul. 2014.
- [3] E. Seifi, M. Atamanesh, and A. K. Khandani, "Media-based MIMO: outperforming known limits in wireless," *Proc. IEEE ICC'2016*, pp. 1-7, May 2016.
- [4] Y. Naresh and A. Chockalingam, "On media-based modulation using RF mirrors," *IEEE Trans. Veh. Tech.*, vol. 66, no. 6, pp. 4967-4983, Jun. 2017.
- [5] Y. Naresh and A. Chockalingam, "A low-complexity maximum-likelihood detector for differential media-based modulation," *IEEE Commun. Lett.*, vol. 21, no. 10, pp. 2158-2161, Oct. 2017.
- [6] A. Bandi, C. R. Murthy, "Structured sparse recovery algorithms for data decoding in media based modulation," *Proc. IEEE ICC'2017*, Jul. 2017.
- [7] B. Shamasundar, A. Chockalingam, "Multiuser media-based modulation for massive MIMO Systems," *Proc. IEEE SPAWC'2017*, Jul. 2017.
- [8] J. Wang, S. Jia, and J. Song, "Generalised spatial modulation system with multiple active transmit antennas and low complexity detection scheme," *IEEE Trans. Wireless Commun.*, vol. 11, no. 4, pp. 1605-1615, Apr. 2012.
- [9] T. Datta and A. Chockalingam, "On generalized spatial modulation," *Proc. IEEE WCNC'2013*, pp. 27162721, Apr. 2013.
- [10] T. Lakshmi Narasimhan and A. Chockalingam, "On the capacity and performance of generalized spatial modulation," *IEEE Commun. Lett.*, vol. 20, no. 2, pp. 252-255, Feb. 2016.
- [11] M. Pretti, "A message passing algorithm with damping," *J. Stat. Mech.: Theory and Practice*, Nov. 2005. doi:10.1088/1742-5468/2005/11/P11008.